Molecular insights into crystallization of minerals: the case of first-row transition metal salt hydrates

Preethi Thomas, Shailabh Tewari, Manisha Jadon, Bharti Singh and Arunachalam Ramanan*

Materials Chemistry Laboratory, Department of Chemistry, Indian Institute of Technology Delhi, New Delhi 110 016, India

How does Nature, the virtuoso chemist, assemble a mineral, an inorganic crystalline compound with a specific composition? How does one account for the directional interactions responsible for the final assembly of a crystal hydrate observed through an X-ray lens? Chemical insights into the aggregation of molecules resulting into simple salt hydrates still evade experimental and theoretical studies. This article gives a perspective of how Nature dictates the structural landscape of MSO_4–H_2O in terms of supramolecular aggregation between the molecular species $\{M(H_2O)_6\}^{2+}$, SO_4^{2-} and H_2O interacting at supersaturation through H-bonding and subsequent coordination forces.

Keywords: Crystallization, hydrogen-bonding, salt hydrates, structural landscape, supramolecular aggregation, topotactic reaction, transition metal.

INTERACTION of molecules steered by the equipoise of attractive and repulsive forces weaves the fabric of genesis as we perceive it. Likewise, the phenomenon of crystallization too embraces this method via molecular recognition leading to self-assembly of chemical species in a supramolecular fashion. In simpler words, supramolecular self-assembly is at the core of crystallization[1]. Nucleation and growth are two significant steps that eventually lead to a crystal from the molecules interacting in the supersaturated region of a solution, otherwise appearing to be homogeneous[2] (Figure 1). However, the fundamental problem of nucleation is that it still lacks molecular insights[3]. What triggers the birth of a crystal nucleus from a supersaturated solution and how could we provide a reliable link between the experimentally observable equilibrium phases demarcated in a phase diagram with a combination of appropriate theoretical models and simulation techniques[4,5]? Recently, there is a growing interest to understand nucleation and growth of the common salt, NaCl and its hydrate, $NaCl{\cdot}2H_2O$ from aqueous media[6]. Additionally, there is significant curiosity about the formation of multidimensional coordination solids such as coordination polymers, metal organic frameworks, etc. in solution[7,8]. Interestingly, most of the relevant studies pay little attention to the structural landscape of a system, i.e. an exhaustive study of the effect of synthetic parameters such as concentration, pH, solvent, temperature, etc. on the formation of a series of related crystal structures with a definite stoichiometry of metal and ligand. For example, no attempt is made to rationalize the composition and structure of the different phases crystallized from even simple systems; such as, NaCl–H_2O, MSO_4–H_2O (M = divalent metal) or copper (or zinc) salt-benzene di/tricarboxylic acid-solvent from aggregating molecular species present in the solution. Twenty-five years ago, Desiraju[8] conceived crystal synthesis of molecular organic solids in terms of supramolecular synthons. The synthons are nothing but supramolecular tools to address the intermolecular interactions at supersaturation. A 'crystal nucleus', a

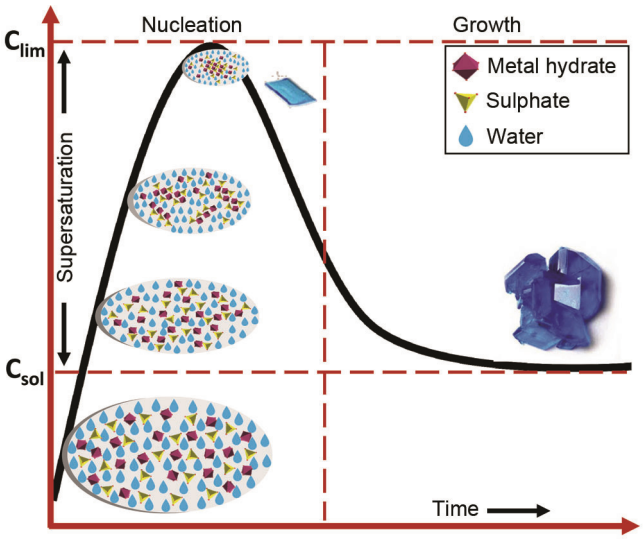

Figure 1. A qualitative plot of concentration versus time for the growth of transition metal sulphate hydrate crystal from solution. The cartoon suggests the building of a crystal nucleus at supersaturation (near maxima) from a set of molecular building blocks directed through noncovalent interactions: copper hydrate complex sulphate ion-pair or 1 : 1 copper sulphate complex.

*For correspondence. (e-mail: aramanan@chemistry.iitd.ac.in)

metastable position is stabilized and grows with a particular habit dictated by forces exerted by the molecules on the surface. In crystal synthesis, the 'crystal nucleus' may be considered equivalent to a supramolecular transition state[8]. Fifteen years ago, Ramanan and Whittingham[9] elucidated the rationale behind formation of selected metal-organic frameworks from condensation of 'point zero charges' or tectons (molecular building blocks) employing retroanalysis of known crystal structures. The 'a posteriori' approach highlighted in their study was extended to several systems containing organic, inorganic and metal–organic species to trace the chemical events from aggregating molecules transforming into a crystal[10–16]. The aggregation of tectons drives the crystal formation onto a supramolecular path leading to the most stable crystal structure, a thermodynamic crystal (global minimum) or a kinetic crystal (local minimum). Two pertinent points to remember here are: If the solid is molecular, then condensation of the molecules in the supersaturated state to form a crystal nucleus is facilitated through weak, noncovalent interactions such as hydrogen-bonding (H-bonding), etc. On the other hand, a nonmolecular solid results when extended metal–ligand coordination (ligand can be neutral like water, amine, etc.) and/or a counter anion (OH^-, X^-, CN^-, SO_4^{2-}, organic anion like multidentate carboxylate or azolate, etc.) favours a stable periodic assembly. A significant feature of this approach is that one can readily recognize the various intermolecular interactions occurring around one or a few metal centres. Also, it becomes obvious to account for the stoichiometry of the overall solid, the environment of the metal and the ligand. In addition, the influence of external factors such as pH, ligand, solvent, counter ion, temperature, etc. becomes evident. It should be noted that the formation of a stable crystal is a compromise between directing intermolecular interactions (coordination, H-bonding, etc.) and close packing (geometry-driven) between aggregating molecules[17].

Nucleation of a metal ion-based solid is invariably centred around a metal complex. Hundred years ago, Werner propounded the concept of coordination theory. It is appropriate to consider that the 'chemically reasonable molecule' which triggers nucleation is a metal complex, a metal hydrate (in aqueous solution) or a metal solvate in its primary coordination sphere; subsequently, other chemical events such as hydrolysis, complexation and/or chelation follow. Crystallization is a kinetic phenomenon and hence the nature of the crystal can dramatically vary depending on the process and other competing molecules present at supersaturation. Though recrystallization is traditionally considered as a purification process for the isolation of organic solids, textbook examples such as benzamide[18] as well as pharmaceutical molecules like aspirin[19] have shown the importance of establishing the monophasic nature of the bulk synthesized product through powder X-ray diffraction technique. Such a verification is crucial because the solids often result in polymorphs and solvates (or hydrates) even with slight variation in the mother liquor. The ternary phase diagram of urea–glutaric acid–water reveals that the stoichiometry of the molecules involved in the isolated crystal may or may not be the same as what is present in the solution[20]. This is equally applicable to inorganic systems as well. However, the metal–ligand coordination poses a major challenge to rationalize the inorganic equivalent of a synthon present in the solution containing metal, with or without organic species in the solution. The exact nature of the molecular species present in the 170-year-old Fehling's solution is still debatable[21]. The above examples highlight the need for rationalizing the formation of a solid in terms of supramolecular aggregation and account for the structural landscape of a system in terms of a conceivable phase diagram. We just observed 2020 as the centenary year of H-bonding[22]. Do we recognize its influence in the isolation of the mineral NaCl above 273 K, the most celebrated salt and the first crystal structure established by the father and son duo, the Braggs in 1913 (ref. 23)? Do we realize that the mineral hydrohalite, $NaCl{\cdot}2H_2O$ precipitates from the same aqueous solution below 273 K (ref. 6)? Its crystal structure was solved as early as 1974 (ref. 24).

A better understanding of the interplaying interactions, particularly coordination forces and H-bonding is a prerequisite for designing metal-based materials with tailor-made functional characteristics. In order to study these forces, we need suitable models to review. Therefore, in an earnest attempt to commence with this endeavour, we turn to Nature, a virtuoso chemist, and examine minerals of simple salts and their hydrates. The study of minerals, which are representative systems of the most stable forms of metal salt hydrates in equilibrium, offers an intriguing view into the thermodynamics and kinetics of building robust inorganic species. The existence of minerals beckons to ask why the so-formed structures with a specific composition are preferred over others. To answer this question, we need to (i) visualize inorganic solids according to their connectivity and stoichiometry and (ii) understand how directional interactions (chemical forces) versus close packing drives crystal formation. A paradigm shift is required on how we designate chemical formulae to inorganic crystals at the molecular level, which truly justifies their structure (geometry, coordination, valency, etc.). Additionally, we need to acknowledge the role of noncovalent interactions, particularly H-bonding in mineral formation. In crystal packing, there is a distinction to be made between coordinated and lattice water. Furthermore, the mineral hydrates are precursors to large inorganic compounds formed through hydrolysis and condensation reactions – a fact that is germane to retroanalysis to trace back the chemical events leading to mineral synthesis. This study is an a posteriori approach on simple mineral sulphate hydrates of divalent first-row transition metals, namely manganese, iron, cobalt, nickel, copper and zinc.

Why transition metal sulphate minerals?

The sulphate minerals of the first-row transition metals exist as hydrates as well as anhydrous forms with comparable crystal structures and show a range of stable solids (equilibrium phases) with similar number of water molecules, thereby providing us a trend to analyse[25]. Moreover, the tetrahedral sulphate with four H-bond acceptors serves an ideal template to examine the directionality for noncovalent interactions with octahedral metal hydrates containing only H-bond donors. This could help us in understanding the extended networks in the structural landscape of the system MSO_4–H_2O. Remember, crystallization can yield molecular solids (zero-dimensional, absence of metal–ligand linkage translating infinitely) or extended metal–ligand interaction along 1D, 2D or 3D. The choice of 3*d* transition metals is due to pronounced electronic changes across the period. On comparison with larger metal ions with diffused orbitals showcasing negligible electronic change effects or *f*-block elements with lanthanide contraction, the effect of change in electronic configuration is conspicuous only for 3*d* metals. These inherent changes in the metal centre are pertinent because they drive the dimensionality of coordination linkages and hence the resultant crystal structure. Magnesium and calcium are *s*-block elements and accommodate more ligands in their coordination sphere comparable to the trend observed in transition metals. Consequently, minerals of Mg and Ca show varied hydration states, their abundance on earth is also quite prominent.

Hydrogen bonding – a directional influence in the crystal engineering of transition metal sulphate hydrates

H-bonding and coordination interactions are the two major interplaying forces of aggregation operating in these salt hydrates. As we know, H-bonding plays a critical role in the structure of DNA, nucleic acids, proteins and water: the elixir of life on earth. In the inorganic realm too, H-bonding drives the crystallization of salt hydrates. The minerals are generally found near a water source, so one can safely assume that their crystallization occurs in aqueous medium. In such an environment, the metal ion gets hydrated and consequently opts for the complementary moieties, i.e. H-bond acceptors to initiate as the product of dehydration reaction of higher hydrate forms, a topotactic reaction. This evident dehydration–hydration reaction serves as the connecting link between the structural landscapes of the entire family of first-row transition metal sulphates. It is interesting to note that as obvious as it might seem, not all hydrates sequentially lose water molecules. It is an anomaly that in nature, heptahydrate form might not necessarily dehydrate to give the hexahydrate form. Thermal stability of the intermediate phases is difficult to predict. The limited data available on the thermal dehydration of various minerals suggests us a peek into the interplaying forces in the M–O–S (M – metal, O – oxygen, S – sulphur) network.

Supramolecular aggregation driven by 1 : 1 metal sulphate complex

In the early stages of crystallization, a metal hydrate can strongly interact with one sulphate ion either through H-bonding forming an ion–pair, $\{M(H_2O)_6\cdots SO_4\}$ or a neutral 1 : 1 complex, $\{M(H_2O)_5(SO_4)\}$. This neutral complex is referred to as point zero charge species[9]. Composition and crystal structures of all the transition metal sulphates (Table 1) observed in the mineral kingdom are of 1 : 1 stoichiometry and the hydrates are of a defined stoichiometry (Table 1). All the structures could be readily visualized by inspecting the aggregation pattern (Figure 2). However, different combinations of H-bonding and coordination forces dictate the way the three molecules, viz. $\{M(H_2O)_6\}^{2+}$, SO_4^{2-} and H_2O condense to optimize a crystal packing with the minimum energy structure in the structural landscape of the MSO_4–H_2O system, similar to what we have observed earlier for the system $CuSO_4$–H_2O (refs 13, 14). Exclusive H-bonding is observed in the case of hepta- and hexa-hydrates (Figures 2 *a*, *b* and 3). Both systems are driven by the tecton, $\{M(H_2O)_6\}\cdots SO_4$ ion–pair. In the former, an additional lattice water per ion-pair is involved to maximize packing, while in the latter H-bonding is dominated between the coordinated water and sulphate oxygens. A mix of the stronger coordination and H-bonding favours the structural arrangement in penta-, tetra- and tri-hydrates. Interestingly, these three hydrates present a contrasting aggregation pattern built of the 1 : 1 tecton, $\{M(H_2O)_5(SO_4)\}$. In the pentahydrate, a strong metal-sulphate coordination extends along 1D and the one lattice water per tecton optimizes the close-packing of the chains through H-bonding. The tetrahydrate is unusual, wherein a pair of 1 : 1 tectons dimerizes to form a discrete cluster $\{M_2(H_2O)_8(SO_4)_2\}$ which further acts as a building block and aggregates through a strong H-bonding. The trihydrate is known only with Cu (Table 1), wherein two coordinated water condenses with two oxygens of the sulphate from two tectons (Figure 2 *e*) to yield the final assembly. Extended coordination through metal-sulphate and metal-aqua is found in monohydrate and the anhydrous metal-sulphate is totally dominated by metal-sulphate coordination.

All six heptahydrate salts are isostructural, except for a change in symmetry (Table 1). In all the salts, apart from the obvious electrostatic force between the metal-hydrate complex and sulphate anion, H-bonding renders directionality and stability to the three aggregating molecular building blocks, viz. $\{M(H_2O)_6\}^{2+}$, SO_4^{2-} and lattice H_2O (Figures 2 and 3). The lattice water acts as both H-bond

Table 1. Crystallographic data for first row transition metal salt hydrates

M(II)	Transition metal sulphate	Space group	a (Å)	b (Å)	c (Å)	α (°)	β (°)	γ (°)	Reference
Mn	$MnSO_4{\cdot}7H_2O$, Mallardite#,¥	$P2_1/c$	14.150	6.500	11.060	90.0	105.60	90.0	28
	$MnSO_4{\cdot}6H_2O$, Chvaleticeite#,¥	$C2/c$	10.050	7.240	24.310	90.0	98.0	90.0	29
	$MnSO_4{\cdot}5H_2O$, Jokokuite#,¥	$P\bar{1}$	6.370	10.770	6.130	98.77	109.97	77.83	30
	$MnSO_4.4H_2O$, Ilesite*,¥	$P2_1/n$	6.020	13.760	8.010	90.0	90.80	90.0	31
	$MnSO_4.H_2O$, Szmikite*,¥	$A2/a$	7.758	7.712	7.126	90.0	115.85	90.0	32
	$MnSO_4$¥	$Cmcm$	5.267	8.046	6.848	90.0	90.0	90.0	33
Fe	$FeSO_4{\cdot}7H_2O$, Melanterite*,¥	$P2_1/c$	14.110	6.510	11.020	90.0	105.25	90.0	34
	$FeSO_4{\cdot}6H_2O$, Ferrohexahydrite^,¥	$C2/c$	10.080	7.280	24.590	90.0	98.3	90.0	35
	$FeSO_4{\cdot}5H_2O$, Siderotil*	$P\bar{1}$	6.260	10.630	6.060	97.25	109.67	75.0	36
	$FeSO_4{\cdot}4H_2O$, Rozenite*,¥	$P2_1/n$	5.945	13.590	7.940	90.0	90.50	90.0	36
	$FeSO_4{\cdot}H_2O$, Szomolnokite*,¥	$A2/a$	7.624	7.468	7.123	90.0	115.87	90.0	37
	$FeSO_4$¥	$Pnma$	8.704	6.801	4.787	90.0	90.0	90.0	38
Co	$CoSO_4{\cdot}7H_2O$, Bieberite#,¥	$P2_1/c$	14.130	6.550	11.000	90.0	105.08	90.0	39
	$CoSO_4{\cdot}6H_2O$, Moorhouseite*,¥	$C2/c$	10.040	7.234	24.300	90.0	98.34	90.0	40
	$CoSO_4{\cdot}4H_2O$, Aplowite#,¥	$P2_1/n$	5.952	13.576	7.908	90.0	90.53	90.0	41
	$CoSO_4{\cdot}H_2O$, Cobalt kieserite~,¥	$C2/c$	6.980	7.588	7.639	90.0	118.65	90.0	42
	$CoSO_4$¥	$Pnma$	8.624	6.715	4.744	90.0	90.0	90.0	43
Ni	$NiSO_4{\cdot}7H_2O$, Morenosite#,¥	$P2_12_12_1$	11.860	12.080	6.810	90.0	90.0	90.0	44
	$NiSO_4{\cdot}6H_2O$, Retgersite*,¥	$P4_12_12$, $P4_32_12$	6.782	6.782	18.280	90.0	90.0	90.0	45
	$NiSO_4{\cdot}H_2O$, Dwornikite*,¥	$C2/c$	6.839	7.582	7.474	90.0	117.85	90.0	46
	$NiSO_4$¥	$Cmcm$	5.155	7.842	6.338	90.0	90.0	90.0	47
Cu	$CuSO_4{\cdot}7H_2O$, Boothite#	$P2_1/c$	14.190	6.537	10.825	90.0	106.02	90.0	48
	$CuSO_4{\cdot}5H_2O$, Chalcanthite#,¥	$P\bar{1}$	6.120	10.700	5.970	97.58	107.17	77.55	49
	$CuSO_4{\cdot}3H_2O$, Bonattite#,¥	Cc	5.590	13.030	7.340	90.0	97.10	90.0	50
	$CuSO_4{\cdot}H_2O$, Poitevinite*	$P\bar{1}$	7.090	7.440	7.820	89.47	119.56	90.45	51
	$CuSO_4$, Chalcocyanite^,¥	$Pnma$	6.690	8.390	4.820	90.0	90.0	90.0	52
Zn	$ZnSO_4{\cdot}7H_2O$, Goslarite#,¥	$P2_12_12_1$	11.818	12.076	6.827	90.0	90.0	90.0	53
	$ZnSO_4{\cdot}6H_2O$, Bianchite*,¥	$C2/c$	10.096	7.201	24.492	90.0	98.27	90.0	54
	$ZnSO_4{\cdot}4H_2O$, Boyleite#	$P2_1/n$	5.950	13.600	7.960	90.0	90.30	90.0	55
	$ZnSO_4{\cdot}H_2O$, Gunningite*,¥	$A2/a$	7.560	7.586	6.954	90.0	115.93	90.0	56
	$ZnSO_4$, Zincosite~,¥	$Pnma$	4.846	6.835	8.699	90.0	90.0	90.0	52, 57
	$ZnSO_4$¥	$F23$	7.176	7.176	7.176	90.0	90.0	90.0	58

*Naturally occurring mineral that is stable at room temperature. #Naturally occurring mineral that dehydrates at room temperature. ^Hygroscopic mineral. ~Mineral whose stability at room temperature is unknown. ¥Synthetic.

donor and acceptor. Geochemists often encounter two major families of heptahydrates among transition metals called as melanterite and epsomite[25]. The monoclinic salts of Mn, Fe, Co, Cu and Zn belong to the former series of minerals, while the orthorhombic salts of Ni and Zn correspond to the latter (Table 1). Note that the Zn salt crystallizes in both monoclinic and orthorhombic forms (polymorphs). The essential difference in their structure is the extent of H-bonding between the sulphate tetrahedron, metal octahedron and lattice water (0D). All the metals, except for copper, form hexahydrates (Table 1). The alternate spatial arrangement of the metal octahedron and sulphate forms the extended H-bonded layer structure. Unlike in heptahydrates, here the hydrogens of the coordinated water only act as donors. Retgersite ($NiSO_4{\cdot}6H_2O$) is an unusual mineral that forms a helix in its extended network crystallizing in a rare enantiomorphic space group, $P4_12_12$.

In pentahydrates, octahedral M(II) centres are coordinated to four water molecules and two sulphate oxygens forming 1D chains of the composition, $\{M(H_2O)_{4/1}(SO_4)_{2/2}\} \equiv [M(H_2O)_4(SO_4)]$ (4/1 means four water molecules are coordinated to one metal ion and 2/2 denotes that two sulphate tetrahedra are shared between two metals) (Figures 2 *c* and 3).

Additionally, one lattice water bridges the chains through H-bonding. The coordinated water molecules act as H-donors in a much similar way as observed in hepta- and hexa-hydrated salts. The bridging sulphates coordinate in a *trans* fashion, and their two oxygens act as H-bond acceptors. In the tetrahydrate system, the metal ion is coordinated to four water molecules and two sulphates (Figure 3). The two non-coordinated oxygens of sulphate exclusively form H-bonds with a pair of water molecules. Interestingly, in this structure a discrete dimer comprising alternating sulphate tetrahedra and metal octahedra interlinked by metal-sulphate coordination bonds. The dimers of the composition $\{M(H_2O)_{4/1}(SO_4)_{2/2}\}_2 \equiv [M(H_2O)_4(SO_4)]$ are H-bonded to each other in the extended network (Figure 2 *d*). In the trihydrate system, the metal cation is coordinated to three different sulphates, while the other three coordinations are provided by three different water

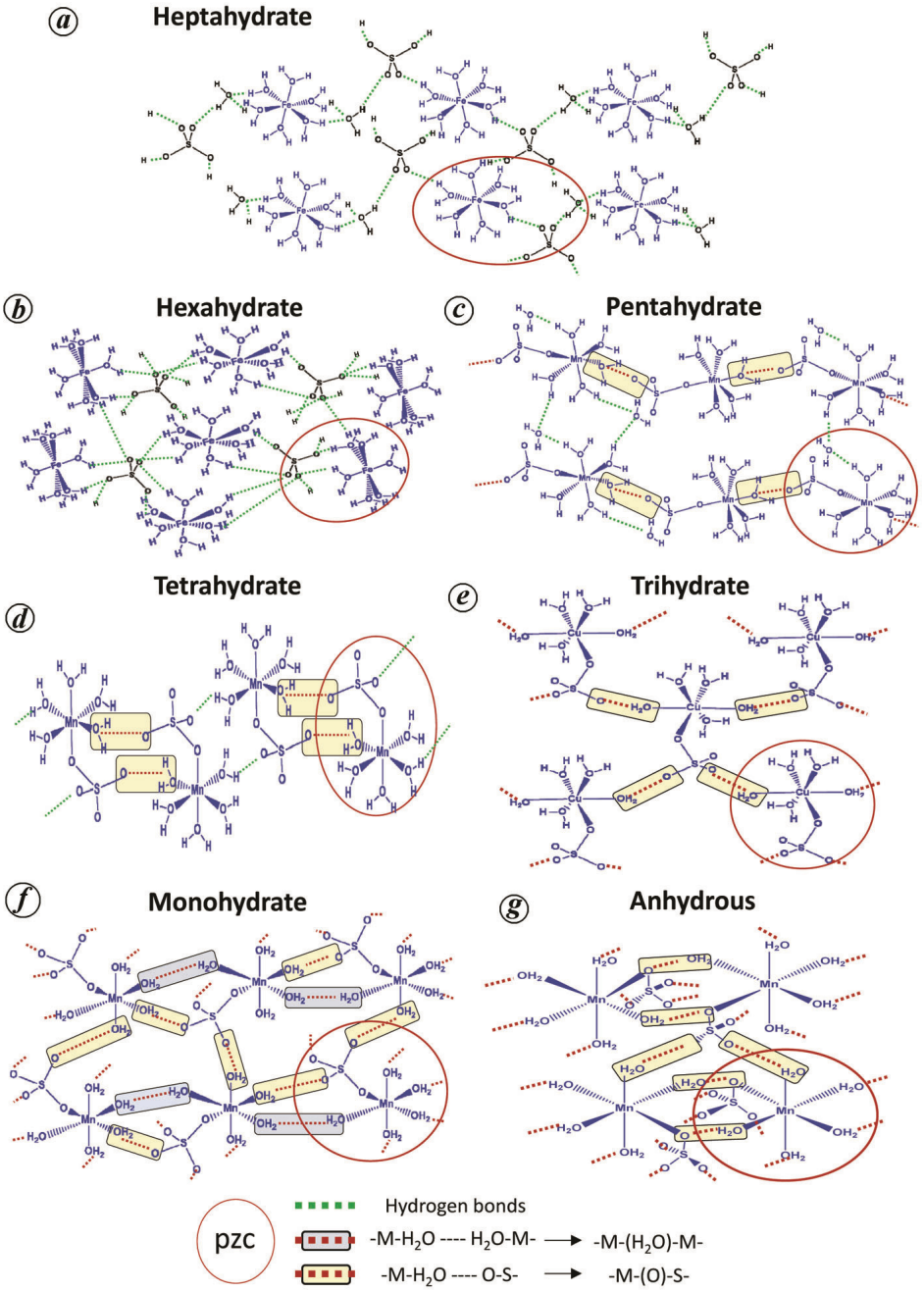

Figure 2. Retroanalysis of the metal sulphate-hydrate system. The diagram depicts the formation of a phase from a neutral and stoichiometric microscopic species that condenses with other such species via H-bonding and coordination linkages leading to the isolation of a metal sulphate-hydrate crystal.

molecules, $\{M(H_2O)_{3/1}(SO_4)_{3/3}\} \equiv [M(H_2O)_3(SO_4)]$. Three of the sulphate oxygens coordinate with the metal, while the fourth oxygen acts as a H-acceptor. The metal-sulphate coordination linkage results in 3D coordination network (Figures 2 *e* and 3).

The monohydrate salts are extensively coordinated both through water and sulphate. The metal is bonded to two water molecules and four sulphate groups (Figure 3). Both water and sulphate bridge adjacent metal centres in an extended 3D coordination network, $[M(H_2O)_{2/2}(SO_4)_{4/4}] \equiv [MSO_4 \cdot H_2O]$. The metal-sulphate monohydrate can be considered as the dehydrated form of its higher hydrated analogues formed through condensation reaction. The anhydrous solid is the final product in the dehydration coupled with condensation $\{M(SO_4)_{6/6}\} \equiv [M(SO_4)]$. Note 6/6 refers to six sulphates being coordinated to a metal ion M and each ligand in turn is coordinated to six metal ions. This notation acknowledges the role of water molecules in forming metal octahedra and the multi-coordination capability of sulphate ligand (Figure 2 *f*).

Topotactic dehydration in the hierarchy of metal salt hydrates

Only limited information is available regarding the thermal behaviour of different hydrated sulphate minerals. Also, not every known mineral hydrate could be successfully crystallized in the laboratory. The system $CuSO_4$–H_2O is the only textbook example wherein transition between the four phases, i.e. penta-, tri-, mono- and anhydrous solids has been successfully achieved either by thermal methods under ambient pressure or varying water vapour pressure at 298 K (refs 25, 26). However, a critical inspection of the structures of all the hydrated and anhydrous metal sulphates suggests a logical pathway for the transformation of higher hydrates to anhydrous salt (Figure 4). Nature beautifully demonstrates the stability of the different hydrated salts through the condensation of metal-sulphate aggregation to successive hydration states culminating in the final anhydrous form, i.e. the lower hydrates retain most of the crystallographic characteristics as their parent hydrate (Figure 3).

Conservation of some of the structural features in the dehydration product could provide us with mechanistic insights into their formation from their precursors. The postulates proposed here provide a clue for unraveling the crystallization jigsaw puzzle. A retroanalysis of the crystal structures of all the phases known in the system MSO_4–H_2O provides a pictorial representation of the 'supramolecular transition state' (Figures 1 and 4), the crucial transient stage just before nucleation at supersaturation. It commences at or in the vicinity of formation of a nucleus via supramolecular aggregation. This subsequently proceeds within the active interface of the precursor hydrate–product hydrate contact zone. Its crystal growth is further facilitated by appropriate reaction conditions at the boundary of the nucleus.

While a hexahydrate can transform into a tetrahydrate which can be facilitated by the elimination of two water molecules from adjacent ion-pairs, penta- to tetrahydrate is unlikely. Also, the transformation of a penta- to trihydrate is viable as elimination of the lattice water followed by the condensing of the adjacent chains through the third oxygen of the sulphate group. Dehydration of a trihydrate to monohydrate is more complex; of the three water molecules, two condense with two water molecules from adjacent metals and the third condenses with sulphate. The subsequent loss of water molecules is accompanied by condensation leading to extended coordination through sulphate ligand. The absence of a dihydrate form may be understood from this dehydration pathway. Only the extensively coordinated $MSO_4 \cdot H_2O$ is formed at the end.

Crystallization and crystal engineering of the mineral salts become more meaningful when the pathway is traced to molecular aggregation[27]. This reaffirms our proposal of topotaxy in dehydration. It ensures preservation of the reaction geometry and structural characteristics of the crystal in the hierarchical family of metal-sulphate hydrates. It is due to H-bonding that the heptahydrate salt is more stable than the hexahydrate form, even though the

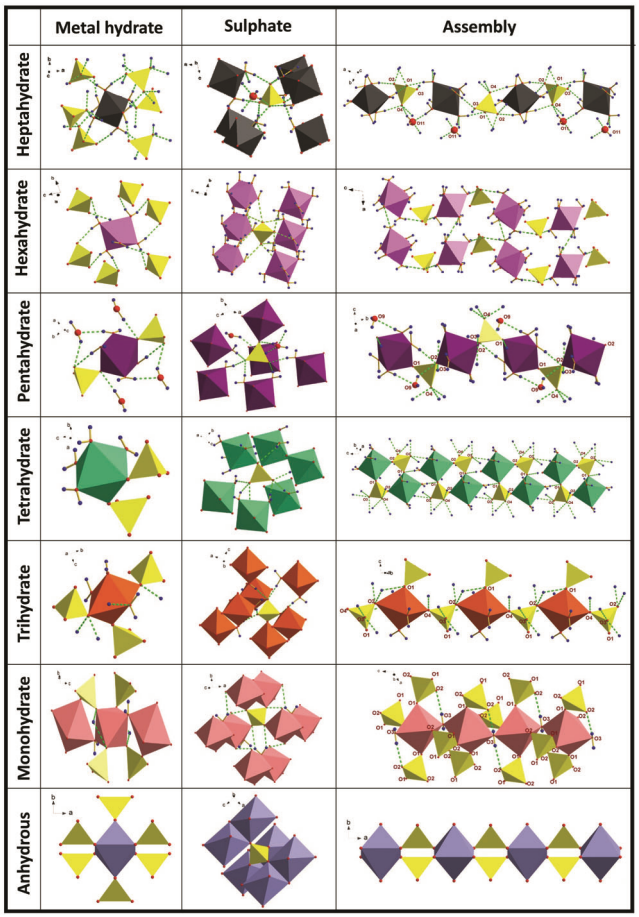

Figure 3. Environment around the metal centre (left), sulphate (centre) and assembly (right) of building blocks into various hydrates.

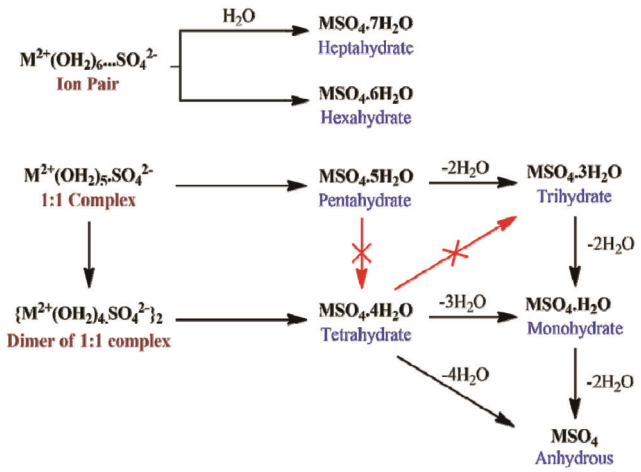

Figure 4. The three 'point zero charged' species (pzc) corresponding to the stoichiometric neutral microscopic species formed at the peak of the concentration versus time plot (Figure 1) crystallizing into different dehydrates.

former has a dispensable lattice water molecule. In fact, in higher hydrate forms H-bonding plays a crucial role in structural stability. Hence, most of the transition metals are found as minerals in the form of heptahydrate in abundance, except copper for which the corresponding mineral boothite is rare owing to distortion-related stability issues. Manganese sulphate exists as tetrahydrate because of the stability rendered by H-bonding.

Conclusion

This perspective emphasizes the need for a paradigm shift in how we perceive structural inorganic chemistry. A clear appreciation of molecular aggregation is required to understand the crystallization of a series of solids based on a metal and ligand from a solvent. The influence of noncovalent interactions in dictating supramolecular aggregation and thus the stoichiometry of a solid with or without the solvent will become apparent. The mechanistic pathway described here could be extended to rationalize the formation of any inorganic or metal organic solid grown from a solution. Retro analysis combined with data mining would provide guidelines to account for the absence of unknown members and devise a synthetic protocol to obtain new solids. Modelling of nucleation will become more meaningful if one integrates crystallization in terms of aggregation of chemically reasonable molecular species. It is difficult to predict why certain minerals are more stable than others under ambient conditions. However, an analysis of the thermal behaviour of higher hydrates to anhydrous forms of the minerals does provide a preview to the topotactic pathway that Nature possibly adopts. The absence of certain hydrates of a particular metal ion reinforces our opinion that both the electronic and geometric structures of the metal complex exert a strong influence in the formation of a periodic array observed in a crystal. This approach is a small step towards better understanding of pre-nucleation stages from a chemical perspective.

1. Desiraju, G., Vittal, J. J. and Ramanan, A., *Crystal Engineering a Textbook*, World Scientific Publishing Company, Singapore, 2011.
2. De Yoreo, J. J. and Vekilov, P. G., Principles of crystal nucleation and growth. *Rev. Mineral. Geochem.*, 2003, **54**, 57–93.
3. Sosso, C., G. C., Chen, J., Cox, S. J., Fitzner, M., Pedevilla, P., Zen, A. and Michaelides, A., Crystal nucleation in liquids: open questions and future challenges in molecular dynamics simulations. *Chem. Rev*., 2016, **116**, 7078–7116.
4. De Yoreo J. J. *et al.*, Crystallization by particle attachment in synthetic, biogenic and geologic environments. *Science*, 2015, **349**, 6760(1–9).
5. Findlay, A. and Campbell, A. N., *The Phase Rule and its Applications*, Longmans, Green and Co, London, UK, 1939, 8th edn.
6. Tsironi, I., Schlesinger, D., Späh, A., Eriksson, L., Segad, M. and Perakis, F., Brine rejection and hydrate formation upon freezing of NaCl aqueous solutions. *Phys. Chem. Chem. Phys.*, 2020, **22**, 7625–7632.
7. Vleet, M. J. V., Weng, T., Li, X. and Schmidt, J. R., *In situ*, time-resolved, and mechanistic studies of metal–organic framework nucleation and growth. *Chem. Rev*., 2018, **118**, 3681–3721.
8. Desiraju, G. R., Supramolecular synthons in crystal engineering – a new organic synthesis. *Angew. Chem. Int. Ed. Engl.*, 1995, **34**, 2311–2327.
9. Ramanan, A. and Whittingham, M. S., How molecules turn into solids: the case of self-assembled metal – organic frameworks. *Cryst. Growth Des*., 2006, **6**, 2419–2421.
10. Upreti, S., Datta, A. and Ramanan, A., Role of nonbonding interactions in the crystal growth of phenazinediamine tetrahydrate: new insights into the occurrence of 2D water layers in crystal hydrates. *Cryst. Growth Des*., 2007, **7**, 966–971.
11. Thomas, J. and Ramanan, A., Growing crystals from solution: by design or by default? *Curr. Sci*., 2007, **93**, 1664–1667.
12. Thomas, J. and Ramanan, A., Growth of copper pyrazole complex templated phosphomolybdates: supramolecular interactions dictate nucleation of a crystal. *Cryst. Growth Des*., 2008, **8**, 3390–3400.
13. Singh, M., Kumar, D., Thomas, J. and Ramanan, A., Crystallization of copper(II) sulfate based minerals and MOF from solution: chemical insights into the supramolecular interactions. *J. Chem. Sci*., 2010, **122**, 757–769.
14. Singh, M., Thomas, J. and Ramanan, A., Understanding supramolecular interactions provides clues for building molecules into minerals and materials: a retrosynthetic analysis of copper-based solids. *Aust. J. Chem*., 2010, **63**, 565–572.
15. Singh, M. and Ramanan, A., Crystal engineering of polyoxomolybdates based metal–organic solids: the case of chromium molybdate cluster-based metal complexes and coordination polymers. *Crystal. Growth Des*., 2011, **11**, 3381–3394.
16. Jadon, M., Srivastava, M., Roy, P. K. and Ramanan, A., From molecules to materials: structural landscape of zinc terephthalates grown from solution. *J. Chem. Sci.*, 2021, **133**(0093), 1–20.
17. Kitaigorodskii, A. I., The principle of close packing and the condition of thermodynamic stability of organic crystals. *Acta Crystallogr*., 1965, **18**, 585–590.
18. David, W. I. F., Shankland, K., Pulham, C. R., Blagden, N., Davey, R. J. and Song, M., Polymorphism in benzamide. *Angew. Chem. Int. Ed. Engl*., 2005, **44**, 7032–7035.
19. Bond, A. D., Boese, R. and Desiraju, G. R., On the polymorphism of aspirin: crystalline aspirin as intergrowths of two 'polymorphic' domains. *Angew. Chem*., *Int. Ed. Engl*., 2007, **46**, 615–617.
20. Chadwick, K., Davey, R. G., Sadiq, G., Cross, W. and Pritchard, R., The utility of a ternary phase diagram in the discovery new co-crystal forms. *CrysEngComm*, 2009, **11**, 412–414.
21. Hörner, T. G. and Klüfers, P., The species of Fehling's solution. *Eur. J. Inorg. Chem*., 2016, **12**, 1798–1807.
22. Gibb, B. C., The centenary (maybe) of the hydrogen bond. *Nature Chem.*, 2020, **12**, 665–667.
23. Bragg, W. H. and Bragg, W. L., The reflection of X-rays by crystals. *Proc. R. Soc. London*, *Ser. A*, 1913, **88**, 428–438.
24. Klewe, B. and Pedersen, B., The crystal structure of sodium chloride dihydrate. *Acta Crystallogr. B*, 1974, **30**, 2363–2371.
25. Hawthorne, F. C., Krivovichev, S. V. and Burns, P. C., The crystal chemistry of sulfate minerals. *Rev. Mineral. Geochem*., 2000, **40**, 1–101.
26. Laidler, K. J. and Meiser, J. H. and Sanctuary, B. C., *Physical Chemistry*, Brooks Cole, Pacific Grove, California, USA, 2002, 4th edn.
27. Sögütoglu, L. C. *et al.*, Understanding the hydration process of salts: the impact of a nucleation barrier. *Crystal. Growth Des.*, 2019, **19**, 2279–2288.
28. Nambu, M., Tanida, K. and Kitamura, T., Mallardite from the Jokoku mine, Hokkaido, Japan. *J. Mineral. Petrol. Sci.*, 1979, **74**, 406–412.
29. Pašava, J., Breiter, K., Huka, M. and Korecký, J., Chvaleticeite, $(Mn,Mg)SO_4{\cdot}6H_2O$, a new mineral. *Neues Jahrb Mineral*., *Monatsh*., 1986, **9**, 121–125.
30. Nambu, M., Tanida, K., Kitamura, T. and Kato, E., Jôkokuite, $MnSO_4{\cdot}5H_2O$, a new mineral from the Jôkoku mine, Hokkaido, Japan. *Mineral. J.*, 1978, **9**, 28–38.

31. Iles, M. W., A new manganese mineral. *Am. Chem. J.*, 1881, **3**, 420–422.
32. Giester, G. and Wildner, M., The crystal structures of kieserite-type compounds. II: crystal structures of $Me(II)SeO_4 \cdot H_2O$ (Me = Mg, Mn, Co, Ni, Zn). *Neues Jahrb. Mineral*., *Monatsh*., 1991, 135–144.
33. Rentzeperis, P. J., Die Kristallstruktur von wasserfreiem $MnSO_4$, und Bemerkungen zur Struktur der beiden $CoSO_4$-Modifikationen. *Neues Jahrb Mineral.*, *Monatsh*., 1958, **1958**, 210–215.
34. Peterson, R. C., The relationship between Cu content and distortion in the atomic structure of melanterite from the Richmond mine, iron Mountain, California. *Can. Mineral*., 2003, **41**, 937–994.
35. Karnitskii, V. A. and Nekrasova, O. I., Secondary minerals of the Nikotovka mercury deposit. *Miner. Res.*, 1930, **1**, 135–138.
36. Jambor, J. L. and Traill, R. J., On rozenite and siderotil. *Can. Mineral*., 1963, **7**, 751–763.
37. Talla, D. and Wildner, M., Investigation of the kieserite–szomolnokite solid–solution series, $(Mg,Fe)SO_4 \cdot H_2O$, with relevance to Mars: crystal chemistry, FTIR, and Raman spectroscopy under ambient and martian temperature conditions. *Am. Mineral.*, 2019, **104**, 1732–1749.
38. Weil, M., The high-temperature β modification of iron(II) sulphate. *Acta Crystallogr. E*, 2007, **63**, i192.
39. Kellersohn, T., Delaplane, R. G. and Olovsson, I., Disorder of a trigonally planar coordinated water molecule in cobalt sulfate heptahydrate, $CoSO_4 \cdot 7D_2O$. *Z. Naturforsch.*, 1991, **B46**, 1635–1640.
40. Zalkin, A., Ruben, H. and Templeton, D. H., The crystal structure of cobalt sulfate hexahydrate. *Acta Crystallogr.*, 1962, **15**, 1219–1224.
41. Kellersohn, T., Structure of cobalt sulfate tetrahydrate. *Acta Crystallogr. C*, 1992, **48**, 776–779.
42. Bechtold, A. and Wildner, M., Crystal chemistry of the kieserite–cobaltkieserite solid solution, $Mg_{1-x}Co_x(SO_4) \cdot H_2O$: well-behaved oddities. *Eur. J. Mineral*., 2016, **28**, 43–52.
43. Wyckoff, R. W. G., *The Structure of Crystals*, Interscience Publishers, Inc., New York, USA, 1951, pp. 40–41.
44. Ptasiewicz-Bak, H., Olovsson, I. and McIntyre, G. J., Charge density in orthorhombic $NiSO_4 \cdot 7H_2O$ at room temperature and 25 K. *Acta Crystallogr.*, 1997, **53**, 325–336.
45. Frondel, C. and Palache, C., Retgersite, $NiSO_4 \cdot 6H_2O$, a new mineral. *Am. Mineral*, 1949, **34**, 188–194.
46. Milton, C., Evans Jr, H. T. and Johnson, R. G., Dwornikite, $(Ni,Fe)SO_4 \cdots H_2O$, a member of the Kieserite Group from Minasragra, Peru. *Mineral. Mag.*, 1982, **46**, 351–355.
47. Dimaras, P. I., Morphology and structure of anhydrous nickel sulphate. *Acta Crystallogr.*, 1957, **10**, 313–315.
48. Leverett, P., McKinnon, A. R. and Williams, P. A., New data for boothite, $CuSO_4 \cdot 7H_2O$, from Burranga, New South Wales. *Aus. J. Mineral*., 2004, **10**, 3–6.
49. Barth, T. F. W. and Tunell, G., The space-lattice and optical orientation of chalcanthite ($CuSO_4 \cdot 5H_2O$); an illustration of the use of the Weissenberg X-ray goniometer in the triclinic system. *Am. Mineral.*, 1933, **18**, 187–194.
50. Jambor, J. L., Second occurrence of bonattite. *Can. Mineral*., 1962, **7**, 245–252.
51. Jambor, J. L., Lachance, G. R. and Courville, S., Poitevinite, a new mineral. *Can. Mineral*., 1964, **8**, 109–110.
52. Kokkoros, P. A. and Rentzeperis, P. J., The crystal structure of the anhydrous sulfates of copper and zinc. *Acta Crystallogr.*, 1958, **11**, 361–364.
53. Anderson, J. L., Peterson, R. C. and Swaison, I. P., Combined neutron powder and X-ray single-crystal diffraction refinement of the atomic structure and hydrogen bonding of goslarite ($ZnSO_4 \cdot 7H_2O$). *Miner. Mag*., 2005, **69**, 259–271.
54. Thorpe, T. E. and Watts, J. I., On the specific volume of water of crystallisation. *J. Chem. Soc.*, 1880, **37**, 102–117.
55. Blake, A. J., Cooke, P. A., Hubberstey, P. and Sampson, C. L., Zinc(II) sulfate tetrahydrate. *Acta Crystallogr. E*, 2001, **57**, i109–i111.
56. Jambor, J. L. and Boyle, R. W., Gunningite, a new zinc sulphate from the Keno Hill–Galena Hill area, Yukon. *Can. Mineral*., 1962, **7**, 209–218.
57. Wildner, M. and Giester, G., Crystal structure refinements of synthetic chalcocyanite ($CuSO_4$) and zincosite ($ZnSO_4$). *Mineral. Petrol*., 1988, **39**, 201–209.
58. Spiess, M. and Gruehn, R., H-$ZnSO_4$, das ersteSulfatmiteinerkubischen H-Cristobalit-Struktur. *Naturwissenschaften*, 1978, **65**, 594–594.

ACKNOWLEDGEMENT. We thank Indian Institute of Technology Delhi for infrastructural and financial support.

Received 6 December 2020; revised accepted 8 November 2021

doi: 10.18520/cs/v122/i1/39-46